Advantages in the Use of Membrane Contactors for the Study of Gas−Liquid and Gas−Liquid−Solid Reactions

Riccardo Tesser,[†] Aldo Bottino,[‡] Gustavo Capannelli,[‡] Fabio Montagnaro,[†] Stefano Vitolo,[†] Martino Di Serio,[†] and Elio Santacesaria*,[†]

Dipartimento di Chimica, Università degli Studi di Napoli Federico II, Complesso Universitario del Monte di Sant'Angelo, 80126 Napoli, Italy, and Dipartimento di Chimica e Chimica Industriale, Università degli Studi di Genova, Via Dodecaneso 31, 16146 Genova, Italy

Laboratory membrane reactors have been studied with the main aim of using such types of devices in kinetic studies of gas−liquid and gas−liquid−solid reactions. As a matter of fact, these reactors allow a better control of the gas−liquid mass transfer phenomena thanks to the absence of emulsions and foams, the interfacial area being constant and stable with different flow rates, and the modular design and ease of scale-up.Four different reactors have been tested to determine what impacts gas absorption from the internal part of the membrane-tube toward the liquid, both in the absence and in the presence of a chemical reaction. In particular, two different agitated reactors have been used: one well-stirred without membranes and the other moderately stirred and containing a coiled bundle of membranes. These two reactors had exactly the same size and stirrer, with the presence of the membrane being the unique difference. The performances of these reactors have been compared for both the physical absorption of oxygen in water and the absorption of oxygen in a sulfite solution containing a cobalt salt. Furthermore, two tubular membrane reactors have been used: one with a single membrane-tube and another one containing a bundle of membrane-tubes. The tubular reactors have been tested in both oxygen physical absorption in water and CO_2 chemical absorption in a solution of NaOH. Finally, an attempt has been made to quantitatively evaluate the effect of very fast chemical reactions on the mass transfer rate in membrane reactors.

Introduction

One of the main aspects in the operation of gas−liquid(−solid) systems is to maximize the rate of the mass transfer phenomena involved by using contactors with the highest interfacial area possible. This can be achieved by working with traditional dispersed phase contactors (such as packed columns, spray towers, bubble tanks, etc.), but the exercise of such devices could involve operational issues. Among them, the presence of dispersed phases could generate emulsions and foams; moreover, unloading and flooding problems could limit the operational range of the contactors, and the interdependence of the fluxes can make the interfacial area variable with the fluid dynamic regime. Finally, a certain density difference must be required if one has to perform a liquid−liquid application. These problems can be substantially avoided by using a nondispersive contact via membrane contactors, as comprehensively surveyed by Armor[1] and Gabelman and Hwang.[2]

The use of membrane contactors has been increasingly affirmed in both the separations field and reactive applications, particularly in the area of gas−liquid reactions.[2,3] These contactors are characterized by a great flexibility and can be employed in a wide range of operating conditions of temperature and pressure, particularly as far as porous ceramic membranes and composite polymeric−ceramic membranes are concerned. Membrane-based contactors are devices that allow a relatively efficient gas−liquid or liquid−liquid mass transfer, without the dispersion of one phase into the other, by means of a microporous membrane, upon the sides of which the two fluids are fluxed. An accurate control of the differential pressure between the two sides of the membrane allows the filling of the pores with one of the fluids in such a way that the contact between the phases is localized at the pore's mouth. With respect to the traditional dispersed phase contactors, this configuration is advantageous from different points of view, such as: (i) the absence of emulsions and foams; (ii) the interfacial area is constant and stable with different flow rates; (iii) the modular design and ease of scale-up; and (iv) the fact that no density difference is required for a liquid−liquid application.

Moreover, membrane-based contactors offer a higher interfacial area and a greater efficiency with respect to those of traditional contactors. The membrane-based gas absorption systems are very efficient and quite easily adaptable to existing plants.[4,5] In addition, extraction processes in membrane reactors have been successfully tested.[6−8] Finally, membrane contactors do not have moving parts, thus allowing the ease of design and scale-up as previously mentioned.[9,10] Nevertheless, membrane systems do also have disadvantages: in some applications, a little higher resistance to the mass transfer[11] was observed, and higher costs related to their finite lifetime are also to be considered. However, membrane contactors are nowadays widely used in industrial chemistry processes.[12−15]

Considering the advantages typical of the membranes, the present work has been focused on the attention to

* To whom correspondence should be addressed. Tel.: +39-081-674027. Fax: +39-081-674026. E-mail: santacesaria@chemistry.unina.it.

[†] Università degli Studi di Napoli Federico II.

[‡] Università degli Studi di Genova.

10.1021/ie050226g CCC: $30.25
Published on Web 06/01/2005

Table 1. Synoptic Scheme of the Experimental Runs Performed

system	absorption	gas phase	liquid phase	gas operation[a]	liquid operation
agitated reactor	physical	air	water	continuous (25 mmHg)	batch (500 mL)
without membranes	chemical	O_2	Na_2SO_3 solution	semibatch (20 mmHg)	batch (500 mL)
agitated reactor	physical	air	water	continuous (15−50 mmHg)	batch (500 mL)
with membranes	chemical	O_2	Na_2SO_3 solution	semibatch (35−55 mmHg)	batch (500 mL)
tubular reactor with a	physical	air	water	continuous (35 mmHg)	continuous (0.01−1.44 mL/s)
single membrane-tube	chemical	CO_2	NaOH solution	continuous (10−90 mmHg)	continuous (0.036−0.1 mL/s)
tubular reactor with a bundle	physical	O_2	water	semibatch (30 mmHg)	continuous (2.45−12.53 mL/s)
of membrane-tubes	chemical	CO_2	NaOH solution	semibatch (30−60 mmHg)	continuous (1.39−4.02 mL/s)

[a] Gas was semibatchwise operated when required by analytical (for agitated reactors) or structural (for multi-tubular reactor) constraints.

the design and on the characterization and testing of membrane-based devices for laboratory investigations in the field of gas−liquid, liquid−liquid, and gas−liquid−solid reactions. The use of a small-scale laboratory reactor, in which the mass transfer operation is carried out by means of a membrane module, represents an interesting device for the following aspects: (i) the screening activity for both catalytic and absorption purposes; (ii) a continuous reactor can more easily be constructed and operated; (iii) the mass-transfer operation zone can be separated from the reaction one; (iv) the interfacial areas are constant and better defined with respect to the mechanically stirred reactors; and (v) the easy development of gas−liquid and gas−liquid−solid lab-scale reactors is useful for screening purposes.

The work has been performed following three different steps. In the first step, a preliminary comparison has been performed between a conventional gas−liquid mechanically agitated reactor and the same device in which the gaseous reactant, flowing in the internal side of a hollow fiber polymeric membrane, was transferred in the liquid phase. Both systems have been tested for the oxygen transfer both in the physical absorption and in the presence of a chemical reaction (sodium sulfite oxidation). A comparison of the performances of the two reactor systems has been made, and a correlation among the stirring rate, the corresponding gas−liquid interfacial area, and the membrane transferring area has been found. The mass transfer performances of the membrane are proportional to the length of the fiber, as demonstrated by runs performed with different amounts of used membrane surface. In a second step of the work, a tubular reactor equipped with a single membrane-tube has been realized and characterized for both pure mass transfer (oxygen in water) and mass transfer in the presence of a chemical reaction (NaOH neutralization with carbon dioxide). This reactor has been operated continuously, with the gas flowing in the inner hole of the membrane fiber while the liquid has been fluxed in the annular space between the membrane and the wall of the cylindrical tube. Runs have been performed in both cases at different liquid flow rates. The model parameters, evaluated from the experimental observations related to this reactor, have also been tested in a scale-up experiment; that is the third step of this work. A similar reactor, equipped with a bundle of membrane-tubes, has been constructed with a scale-up factor of >30 (with respect to the membrane interfacial area) when compared to the reactor with a single membrane-tube. This multi-tubular reactor, like the previous one, has been used in both pure physical absorption (oxygen in water) and absorption with chemical reaction (CO_2 in NaOH solution). The results of the scale-up experiments were successful because the mass transfer parameters, evaluated with the single-tube reactor, can be transferred to the higher scale (i.e., to a multi-tubular reactor having a higher number of membrane-tubes), keeping a satisfactory agreement between experiments and calculations.

In the different mentioned reactors, mass transfer rates for physical absorption and absorption in the presence of a very fast reaction were compared, with the aim of verifying the effect of the chemical reaction. For this purpose, it is interesting to observe that a very fast reaction strongly increases the gas pressure drop ΔP necessary for observing incipient formation of gas bubbles on the external surface of the membrane. These ΔP values, therefore, seems strictly correlated with the enhancement factor.

For all the experimental setups, suitable mathematical models have been developed as tools for the description of collected data. Model calculations and experimental data are in good agreement. The developed membrane-based lab-scale reactors can easily be constructed and continuously operated, allowing both a rapid screening of a mass-transfer-limited gas−liquid reaction and a more detailed and rigorous kinetic study. The experimental data can be more easily collected within these devices because of the more accurate control on the mass-transfer operation, when compared with data obtained in the conventional mass-transfer contacting devices where the interfacial areas are affected by many different factors. Finally, by using membranes, a miniaturization of gas−liquid and gas−liquid−solid reactors is possible.

Apparatus, Reagents, and Methods

In this section, the details of the experimental tests will be given. A synoptic scheme of the experimental runs performed (in all cases at room temperature) is reported in Table 1. As can be seen, there were differences in the operating conditions, mainly concerning the nature of the gas phase to absorb, as well as the gas and the liquid feeding modalities. This was due to experimental conveniences and/or structural constraints. However, these differences were opportunely taken into account in both experimental results processing and their discussion.

Membrane Properties. The hollow membrane used in this work was a microporous polypropylene capillary membrane Akzo Nobel Accurel PP S6/2 supplied by Membrana Co. The membrane was investigated under a Leo Stereoscan 440 SEM, with accelerating voltages of 10 and 20 kV and magnifications ranging from 15 000x to 150 000x. Dried membrane samples were fixed to an SEM spin stub with a conductive adhesive and then coated with a 20 nm layer of gold using a sputtering device (AGAR PS3). The SEM investigation on this material (Figure 1) gave the following main results for the membrane-tube: inner diameter = 1.8 mm and wall thickness = 0.45 mm. The mean pore size, as supplied by the membrane furnisher, is 0.2 μm.

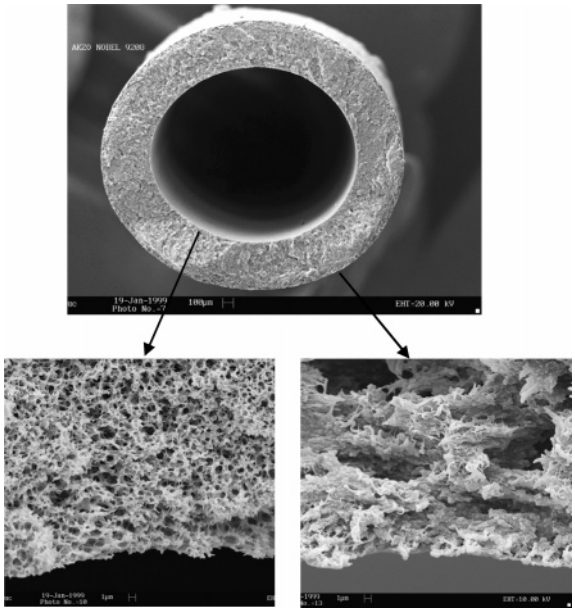

Figure 1. SEM micrograph of the section of the hollow microporous polypropylene capillary membrane employed.

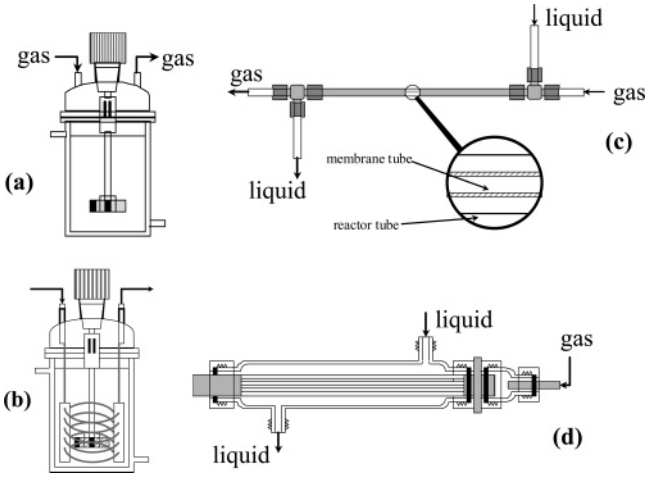

Figure 2. Sketch of the experimental apparatus employed (not to scale): (a) agitated reactor without membranes; (b) agitated reactor with membranes; (c) tubular reactor with a single membrane-tube; (d) tubular reactor with a bundle of membrane-tubes.

Description of the Employed Reactors. Four different types of reactors were employed in performing the runs listed in Table 1 (schematically depicted in Figure 2). As can be seen, two different agitated reactors were used: one well-stirred (Figure 2a) and the other moderately stirred (Figure 2b) and containing a coiled bundle of membranes. These two reactors have exactly the same size and stirrer, with the presence of the membrane being the unique difference. Furthermore, two tubular membrane reactors were used: one with a single membrane-tube (Figure 2c) and another containing a bundle of membrane-tubes (Figure 2d).

Agitated Reactors. The system (Figure 2a and b) was a cylindrical glass-jacketed reactor (volume $\approx$ 500 mL) equipped with a hollow steel stirrer (connected to a motor able to vary its rounds per minute, rpm). Thermostated water was fluxed to the reactor jacket in order to maintain the system isotherm. The gas entered the head of the reactor; its flow was controlled by a valve, and the pressure was read by a Hg manometer able to give the pressure difference, ΔP, between the inlet gas and the reactor, kept constant at 1 atm. The gas was sucked into the hollow stirrer by means of properly designed holes on its top. Then it passed through the stirrer, exiting from the holes on its bottom, thus entering the liquid phase. The tests were conducted batchwise with respect to the liquid phase; the gas phase flowed continuously in the physical absorption tests, while in the chemical absorption tests, the gas was semibatchwise fed (the gas outlet of the reactor was plugged).

The agitated reactor with membranes was equipped with a coil of 4 or 6 membrane-tubes (length = 54 cm each), separated from each other by a Teflon framework. The gas entered the membrane system and was transferred to the liquid phase through the membranes' surfaces. The stirrer still worked, but in a nitrogen atmosphere without the formation of gas bubbles. Also in this case, the liquid was batchwise operated, and the gas was operated either continuously (in the case of physical absorption) or not (in the case of chemical absorption, with the membrane outlet, in this case, being plugged).

Physical absorption tests were conducted by using technical grade air as the gas phase and bidistilled water as the liquid phase. In every test, water was appropriately deoxygenated by an N_2 stream, which in turn allowed the water to be considered N_2-saturated and allowed the further N_2 absorption to be neglected. Chemical absorption tests were conducted by using O_2 (supplied in cylinders by Son Co.) as the gas phase and a solution of water$-Na_2SO_3$ (0.5 M)$-CoSO_4 \cdot 7H_2O$ (5.5×10^{-3} M) as the liquid phase. The sodium sulfite reactant and the catalyst (cobalt sulfate heptahydrate) were both supplied as solids by Fluka at the maximum level of purity available ($\geq$98.0% for Na_2SO_3 and $\geq$97.5% for the catalyst). In the runs performed with the membranes, the ΔP corresponding to the incipient bubbles formation was preliminarily evaluated in order to find the best operating conditions.

When the agitated reactor without membranes is considered, in physical absorption tests, 500 mL of water was put into the reactor in which air was fed at a flow rate corresponding to ΔP = 25 mmHg. The tests were conducted at stirring rates ranging from 200 to 600 rpm. An amperometric electrode (equipped with an Au microelectrode) was put into the reactor with the aim of measuring the oxygen concentration in the liquid phase as a function of time. Concentration signals were logged on a PC at a sampling rate of 1 Hz. In chemical absorption tests, first of all, a range of operating conditions was found in which kinetics is not dependent on Na_2SO_3 and catalyst concentration and the reaction takes place at the gas$-$liquid interface. Then, 500 mL of liquid solution was put into the reactor. Pure oxygen was fed to the system (ΔP = 20 mmHg) with the aim of investigating the catalytic reaction

$$Na_2SO_3 + {}^1/_2O_2 \xleftarrow{CoSO_4 \cdot 7H_2O} Na_2SO_4 \qquad (1)$$

whose detailed mechanism and kinetics have been largely described in the literature.[16] The tests were conducted at stirring rates ranging from 450 to 600 rpm. The lowest stirring rate was chosen as the reference test, in which no bubble and vortex formation was observed in the reactor and the specific interfacial area a_{ref} could be simply defined as the ratio section/volume of the reactor ($a_{ref} = 0.11\ cm^{-1}$). In this test, the rate of

oxygen chemically absorbed N_{ref} was deduced by reading the value of the O_2 flux by a flowmeter located at the inlet of the reactor. In fact, since the operating conditions were such as to work in a fast kinetic regime and with a large Na_2SO_3 excess, this flux was estimated as equal to that consumed in the liquid system by chemical absorption (it is recalled here that the gas outlet was plugged). Higher stirring rates were able to generate higher interfacial areas a_i, which were calculated employing the simple relation[16]

$$\frac{a_i}{a_{ref}} = \frac{N_i}{N_{ref}} \tag{2}$$

where N_i is the rate of oxygen chemically absorbed at a fixed stirring rate. It must be pointed out that a_i is an apparent interfacial area, because the mass transfer coefficient also changes along with the stirring rate; accordingly, the values of the mass transfer coefficient determined in the reference conditions were arbitrarily assumed as constant, as better specified in the Results.

When the agitated reactor with membranes is considered, quite similar procedures were followed. As far as physical absorption tests are concerned, the differences with respect to the tests in the reactor without membranes were (a) stirring rates were in the range 200−500 rpm and (b) the air was fed at a ΔP ranging from 15 to 50 mmHg. In chemical absorption tests, the differences were (a) the stirring rate was fixed at 450 rpm and (b) the oxygen was fed at a ΔP ranging from 35 to 55 mmHg. Finally, in chemical absorption tests, the membranes were closed at one extremity and pure oxygen was fed with a flow rate exactly corresponding to the absorption rate.

Tubular Reactors. As far as the tubular reactor with a single membrane-tube is concerned (Figure 2c), it was a stainless steel tube with an internal diameter of 4.8 mm in which a single membrane-tube (17 cm length) was located. The specific geometric interfacial area of the membrane, expressed as the ratio between the external surface area of the membrane-tube and the liquid volume, was 6.86 cm^{-1}. This reactor was used for physical absorption tests. A similar glass reactor (i.d. = 9.4 mm, length of the membrane-tube = 21.5 cm, specific geometric interfacial area of the membrane = 1.33 cm^{-1}) was used for chemical absorption tests. These two tubular reactors are characterized by different values of the specific geometric interfacial area, to evaluate the influence of this parameter on the reactor performance. Liquid continuously flowed into the annulus (volume = 2.10 mL for the physical tests and 13.7 mL for the chemical tests) by means of a piston pump; gas continuously flowed into the membranes.

As far as the tubular reactor with a bundle of membrane-tubes (Figure 2d) is concerned, it was a glass tube in which a bundle of 35 membrane-tubes (length = 17 cm each) plugged at one extremity was located. Liquid continuously flowed into the shell (volume = 135 mL) by means of a peristaltic pump; gas was semibatchwise fed into the bundle.

As far as the tubular reactor with a single membrane-tube is concerned, physical absorption tests were conducted with a water flow rate ranging from 0.01 to 1.44 mL/s and an air flow rate corresponding to ΔP = 35 mmHg. The electrode system was able to measure the oxygen concentration in the outlet liquid. Chemical absorption tests were conducted by using CO_2 (supplied in cylinders by Son Co.) as the gas phase and a solution of water−NaOH (1 M) as the liquid phase. Sodium hydroxide was supplied as a solid by Aldrich. In these tests, a liquid flow rate ranging from 0.036 to 0.1 mL/s and a CO_2 flow rate corresponding to ΔP ranging from 10 to 90 mmHg were employed, to investigate the behavior of the reaction

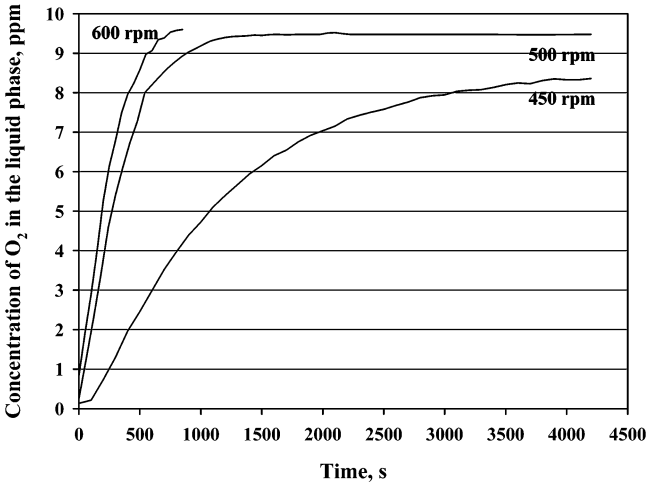

Figure 3. Trends of $C^L_{O_2}(t)$ for tests of the physical absorption of O_2 into water in the agitated reactor without membranes at different stirring rates (ΔP = 25 mmHg).

$$2NaOH + CO_2 \leftrightarrow Na_2CO_3 + H_2O \tag{3}$$

The outlet liquid was titrated with a standard solution of HCl (1 M) in order to measure the unconverted OH^- concentration.

In the case of the tubular reactor with a bundle of membrane-tubes, physical absorption tests were conducted by using pure O_2 as the gas phase and water as the liquid phase. Chemical absorption tests were conducted by using CO_2 as the gas phase and a solution of water−NaOH (0.86 M) as the liquid phase. In physical absorption tests, the differences with respect to the previous case were (a) the water flow rate ranged from 2.45 to 12.53 mL/s and (b) the O_2 was semibatchwise fed at ΔP = 30 mmHg. In chemical absorption tests, the differences were (a) the liquid flow rate ranged from 1.39 to 4.02 mL/s and (b) the CO_2 was semibatchwise fed at a ΔP ranging from 30 to 60 mmHg.

Results

Agitated Reactors. First of all, physical absorption tests of O_2 into a batch of water were conducted in the agitated reactor without membranes (Figure 2a) at different stirring rates (200−600 rpm). The aim of these runs is to measure the oxygen absorption rates, useful when considering the tests performed in a similar reactor in which physical absorption occurs via the membranes (Figure 2b). In the experimental runs performed in the range 200−450 rpm, absorption rates were poorly affected by stirring rate, because no bubbles and vortexes were formed in the system: 450 rpm is, therefore, the threshold value for the development of interfacial contact area. Figure 3 reports the time evolution of the concentration of O_2 dissolved in water, $C^L_{O_2}(t)$, for stirring rates of 450, 500, and 600 rpm, respectively. The plots of Figure 3 can be interpreted by using the following mass transfer balance equation

$$\frac{dC^{L}_{O_2}(t)}{dt} = k_L a[C^{*,L}_{O_2} - C^{L}_{O_2}(t)] \quad (4)$$

where $C^{*,L}_{O_2}$ is the concentration of O_2 at equilibrium (i.e., the saturation value) and $k_L a$ is the product between the mass transfer coefficient in the liquid phase k_L (cm/s) and the specific liquid/gas interfacial area a (cm^{-1}). The initial condition of this differential equation is $C^{L}_{O_2}(t=0) = 0$, and its solution can be expressed as

$$\ln\left(\frac{C^{*,L}_{O_2}}{C^{*,L}_{O_2} - C^{L}_{O_2}(t)}\right) = k_L a t \quad (5)$$

By plotting the left-side member of eq 5 as a function of time, straight lines are obtained with slopes that give the values of the overall volumetric mass transfer coefficient $\beta_L = k_L a$. The β_L value obtained at the reference stirring rate (450 rpm) allows one to calculate a k_L value (9.3×10^{-3} cm/s) once the reference interfacial area at 450 rpm is fixed (0.11 cm^{-1}). Generally speaking, β_L is a function of both k_L and interfacial area a. By neglecting the influence of the stirring rate on k_L, and thus assuming it constant at 9.3×10^{-3} cm/s, the values of β_L obtained at 500 and 600 rpm allow one to calculate the corresponding apparent interfacial area values, which increase as the stirring rate increases (Table 2). In this assumption, the observed variation of β_L with the stirring rate is entirely ascribed to the interfacial area a.

Different runs of the chemical absorption of oxygen in a sodium sulfite solution containing $CoSO_4$ as the catalyst were performed in the same reactor. As is well-known, this reaction (eq 1) is extremely fast provided that opportune experimental conditions related to the sulfite and catalyst concentration are respected.[16] In this case, oxygen absorption occurs more rapidly than in a simple physical absorption, thanks to the enhancement of the mass transfer induced by the chemical reaction. However, the enhancement factor remains constant along with the stirring rate, and this method is, therefore, generally adopted for the measurement of the specific interfacial area. In Table 3, the absorption rates obtained for different stirring rates are reported. By comparing the absorption rates evaluated at 500 and 600 rpm with the one obtained at 450 rpm, it is possible to evaluate the apparent specific interfacial area for any stirring rate (Table 3 and eq 2). It is interesting to observe that the values of the specific interfacial area reported in Tables 2 and 3 are in good agreement, also considering that, in the runs performed with sulfite, pure O_2 instead of air was employed. As an order-of-magnitude comparison, the rate of O_2 physically absorbed in the reactor at 500 rpm can be evaluated as the product between $k_L a$ and the initial concentration driving force in the liquid phase, and its result is $\sim 6.9 \times 10^{-7}$ mol/(s·L of liquid phase). At the same stirring rate in the chemical absorption, the values of N and of the volume of the liquid phase give $\sim 2.89 \times 10^{-4}$ mol/(s·L of liquid phase). The ratio between these two values, with the rate of O_2 physically absorbed opportunely normalized to an ideal case in which pure O_2 instead of air was present, gives an enhancement factor of ~84. The same calculation at 600 rpm gives an enhancement factor of 89.

Subsequently, similar runs have been performed in the agitated reactor with membranes shown in Figure 2b. Oxygen physical absorption results are reported in Figure 4 for 400 rpm and $\Delta P = 35$ mmHg (the coil of 4 membrane-tubes was employed); the results obtained at 500 rpm were quite similar. The behavior does not depend on the stirring rate, because the latter does not affect mass transfer which occurs through the membranes: the use of membranes requires a moderate stirring for renewing the liquid near the membrane surface. Another important condition in the use of membranes is the ΔP of the gas to be used in the runs: the ΔP must be chosen as the limit value at which incipient gas bubbles are formed. In this case, this value was $\Delta P \approx 35$ mmHg. In Figure 5 the calculated values for β_L (see eq 5) in different operating conditions are reported. As can be seen, at a fixed ΔP, stirring rates affect β_L values until the threshold value of 400 rpm is reached, and then β_L remains almost constant. A correct value of k_L for the membranes can, therefore, be calculated by considering only β_L values determined for $\Delta P \approx 35$ mmHg and for an average stirring rate of 450 rpm. Moreover, runs in this type of reactor have been made by using a coil of 4 or 6 membrane-tubes having the same geometrical and physical properties. By increasing the number of membrane-tubes from 4 to 6, the β_L value increases in a quite proportional fashion from $\sim 1.3 \times 10^{-3}$ s^{-1} to $\sim 2.2 \times 10^{-3}$ s^{-1} (Figure 5). The tests with a coil of 6 membrane-tubes have been performed at the average stirring rate of 450 rpm, since the tests with a coil of 4 membrane-tubes have shown no significant differences for the β_L values when the stirring rate has increased from 400 to 500 rpm. The

Table 2. Results for Tests of the Physical Absorption of O_2 into Water in the Agitated Reactor without Membranes at Different Stirring Rates

ΔP (mmHg)	stirring rate (rpm)	β_L (s^{-1})	a (cm^{-1})
25	450	1.02×10^{-3}	0.11 (a_{ref})
25	500	2.32×10^{-3}	0.25
25	600	4.18×10^{-3}	0.45

Table 3. Results for Tests of the Chemical Absorption of O_2 into a Na_2SO_3 Solution in the Agitated Reactor without Membranes at Different Stirring Rates

ΔP (mmHg)	stirring rate (rpm)	N (mL/s)	a (cm^{-1})
20	450	1.67 (N_{ref})	0.11 (a_{ref})
20	500	3.47	0.23
20	600	6.67	0.44

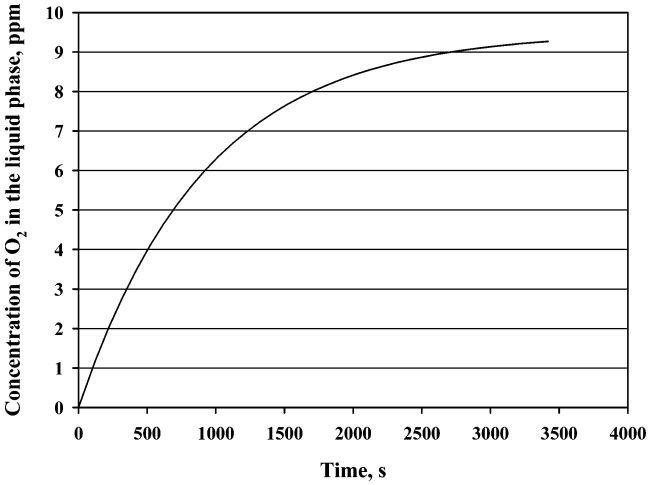

Figure 4. Trend of $C^{L}_{O_2}(t)$ for tests of the physical absorption of O_2 into water in the agitated reactor with membranes (stirring rate = 400 rpm; $\Delta P = 35$ mmHg; coil of 4 membrane-tubes).

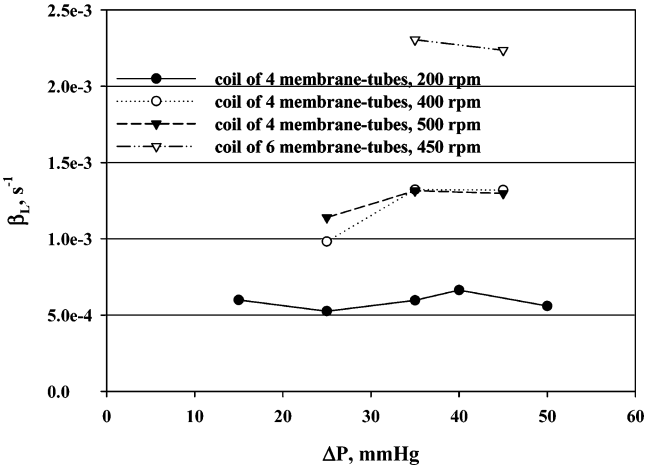

Figure 5. Overall mass transfer coefficient β_L as a function of ΔP for tests of the physical absorption of O_2 into water in the agitated reactor with membranes at different stirring rates and coils of membrane-tubes.

Table 4. Rate of O_2 Chemically Absorbed into a Na_2SO_3 Solution in the Agitated Reactor with Membranes at Different ΔP's of the Gas Feed

ΔP (mmHg)	stirring rate (rpm)	N (mL/s)
35	450	3.19
40	450	3.19
45	450	3.33
55	450	3.47

knowledge of β_L allows one to calculate the interfacial area values, once the reference k_L value (obtained for the system without membranes) is fixed at 9.3×10^{-3} cm/s. Moreover, dividing this area by the specific surface of the membrane coil, expressed as the ratio between the external surface area of the membrane coil and the liquid volume, yields a value for the membrane surface porosity of ~0.36, which is in good agreement with the value supplied by the membrane furnisher for the overall porosity (0.31).

The agitated reactor containing a coil of 6 membrane-tubes has then been used for performing sodium sulfite oxidation experiments. A breakthrough pressure was observed for the incipient bubble formation of at least 55 mmHg, well higher than that (35 mmHg) measured when physical absorption tests were performed in this reactor. This means that, in the presence of a very fast chemical reaction, mass transfer rates are also enhanced in the membrane contactors and this occurs by directly affecting the breakthrough ΔP value. In Table 4 it can be seen that by increasing the ΔP from the previously determined value of 35 mmHg to the new breakthrough value of 55 mmHg the mass transfer rate correspondingly increases. A selection of the most interesting results obtained for the specific interfacial area when working with the agitated reactor with and without membranes is reported in Figure 6. In this figure, the black circles are related to the agitated reactor without membranes. It is clearly observed that, in this device, 450 rpm is a threshold value for the development of interfacial area by stirring. Then, it can be observed (cf. hollow circles) that the agitated reactor with a coil of 4 membrane-tubes (when physical absorption is considered) is almost equivalent, in terms of the specific interfacial area and in the range ~470−500 rpm, to the agitated reactor without membranes (the value of a is in the range 0.11−0.15 cm^{-1}). Also in this case, a value for the enhancement factor was found by comparing the

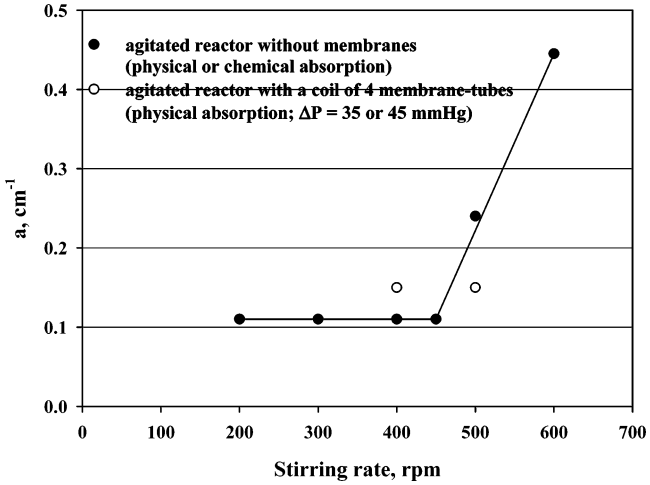

Figure 6. Specific interfacial area as a function of the stirring rate for tests conducted in the agitated reactor under different operating conditions.

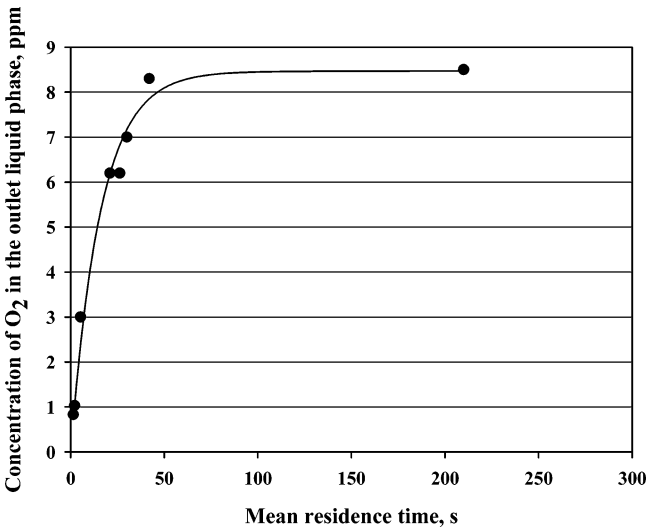

Figure 7. Values of outlet $C^L_{O_2}$ for tests of the physical absorption of O_2 into water in the tubular reactor with a single membrane-tube as a function of the water mean residence time in the annulus (ΔP = 35 mmHg).

rate of O_2 physically absorbed with that of O_2 chemically absorbed: these values were similar when compared with those obtained in the reactor without membranes; thus, the enhancement factor resulted again in the range 85−90.

Tubular Reactor with a Single Membrane-Tube. Two tubular reactors differing in the length of the membrane-tube and in the size of the annulus have been used. The two reactors have, therefore, different values of the specific interfacial membrane area. Figure 7 reports the experimental results of physical absorption tests, expressed in terms of $C^L_{O_2}$ (concentration of O_2 dissolved in the outlet water at steady state) as a function of the water mean residence time ($\bar{t}$) in the annulus. These runs were carried out in the tubular reactor with a specific geometric interfacial area of 6.86 cm^{-1}. It can be observed that the lower the $\bar{t}$ value(i.e., the higher the water flow rate), the lower the C^L_{O2} value, which decreases rather abruptly from 8.5 ppm (at $\bar{t} \approx 3.5$ min) to 0.8 ppm (at $\bar{t} < 2$ s). To estimate the mass transfer coefficient, the following differential equation was considered

$$u^{\mathrm{L}} \frac{\mathrm{d}C^{\mathrm{L}}_{\mathrm{O}_2}(z)}{\mathrm{d}z} = k_{\mathrm{L}}a[C^{*,\mathrm{L}}_{\mathrm{O}_2} - C^{\mathrm{L}}_{\mathrm{O}_2}(z)] \tag{6}$$

with boundary condition $C^{\mathrm{L}}_{\mathrm{O}_2}(z=0) = 0$ and with the expression of the concentration profile of the dissolved oxygen as a function of the reactor axis z. In eq 6, u^{L} is the axial velocity of the liquid-phase flowing in the annulus, while $C^{*,\mathrm{L}}_{\mathrm{O}_2}$ is the saturation value of the oxygen concentration in the liquid phase, taken to be 8.5 ppm (see Figure 7). One particular solution of eq 6 is for $z = z_{\mathrm{L}}$ (i.e., at the reactor outlet),

$$\ln\left(\frac{C^{*,\mathrm{L}}_{\mathrm{O}_2}}{C^{*,\mathrm{L}}_{\mathrm{O}_2} - C^{\mathrm{L}}_{\mathrm{O}_2}(z_{\mathrm{L}})}\right) = k_{\mathrm{L}}a\frac{z_{\mathrm{L}}}{u^{\mathrm{L}}} = k_{\mathrm{L}}a\,\bar{t} \tag{7}$$

which is able to give the values for $\beta_{\mathrm{L}} = k_{\mathrm{L}}a$. By exploiting the experimental results, β_{L} turned out to be $\sim 5 \times 10^{-2}$ s^{-1}, higher than the values obtained for the physical absorption in the agitated reactor with membranes (cf. Figure 5). This can be explained by considering the small volume of the liquid flowing in the annulus, which increases the value of the specific area.

Chemical absorption tests of CO_2 in 1 M NaOH solution have been performed in the membrane reactor having a specific interfacial area of 1.33 cm^{-1}. The unconverted OH^- concentrations in the outlet liquid were rearranged in terms of a degree of OH^- conversion

$$x = \frac{C^0_{\mathrm{OH}^-} - C_{\mathrm{OH}^-}(z_{\mathrm{L}})}{C^0_{\mathrm{OH}^-}} \tag{8}$$

where $C^0_{\mathrm{OH}^-}$ is the OH^- concentration in the inlet liquid. Experimental tests were performed at different liquid mean residence times $\bar{t}$ and at different ΔP's of CO_2. In Figure 8, OH^- conversion as a function of the ΔP applied to the CO_2 reagent for different residence times t is reported. As can be seen, the conversion is affected in a complex way by both ΔP and residence time. To describe in detail all the observed behaviors, it is necessary to develop a mass transfer model considering also the concentration profiles inside the pores: this will be the subject of a further development of this work. Following the simplified approach previously described, the attention was focused only to the runs performed at a ΔP corresponding to incipient bubbles formation, in which the pores are almost completely filled with gas. It must be pointed out, first of all, that in the presence of an extremely fast reaction, such as that of CO_2 with NaOH, the ΔP for incipient bubbles formation is in the range 60−90 mmHg, according to the liquid flow rates from 0.036 to 0.1 mL/s. The ΔP values obtained are much higher than those obtained in the physical absorption. This aspect suggests that the ΔP for incipient bubbles formation is strongly related to the enhancement factor.

To estimate the enhancement factor of this reaction, the rate of CO_2 chemically absorbed, measured at a ΔP corresponding to the incipient bubbles formation, can be compared with that of oxygen physically absorbed in a similar tubular reactor, by taking into account the difference in both the used gas partial pressures and the O_2−CO_2 diffusion coefficients. The calculus of the mass transfer coefficient, in the case of chemical absorption, may be performed by considering that the decrease in OH^- concentration along the z-axis is equal to 2 times

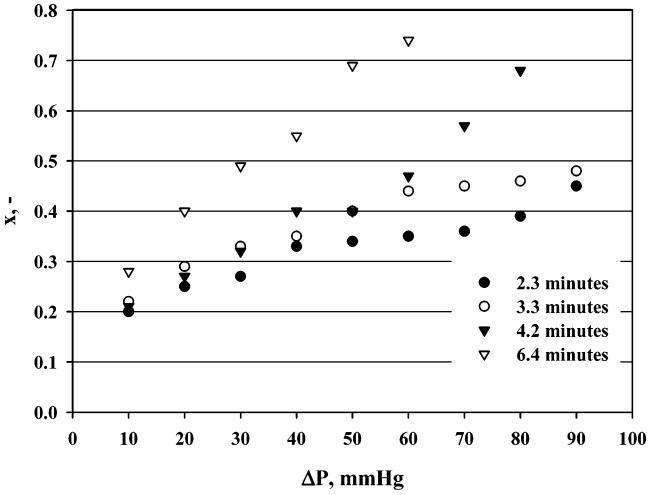

Figure 8. Values of x for tests of the chemical absorption of CO_2 into a NaOH solution in the tubular reactor with a single membrane-tube as a function of the gas ΔP and the liquid mean residence time in the annulus.

the CO_2 mass transfer into the liquid phase (see eq 3), if a very fast reaction is assumed,[17]

$$-u^{\mathrm{L}} \frac{\mathrm{d}C_{\mathrm{OH}^-}(z)}{\mathrm{d}z} = 2k_{\mathrm{L}}aC^{*,\mathrm{L}}_{\mathrm{CO}_2} \tag{9}$$

where $C^{*,\mathrm{L}}_{\mathrm{CO}_2}$ is the saturation value of the carbon dioxide concentration in the liquid phase (4.4×10^{-2} M), taken from literature data[18] and, under the assumption that all the CO_2 transferred into the liquid phase reacts with NaOH, this last actually being in excess with respect to CO_2 in the operating conditions adopted (i.e., the driving force of the CO_2 mass transfer into the liquid phase is $C^{*,\mathrm{L}}_{\mathrm{CO}_2} - 0$). From eq 8, eq 9 can be rewritten as

$$u^{\mathrm{L}}C^0_{\mathrm{OH}^-} \frac{\mathrm{d}x(z)}{\mathrm{d}z} = 2k_{\mathrm{L}}aC^{*,\mathrm{L}}_{\mathrm{CO}_2} \tag{10}$$

with boundary condition $x(z=0) = 0$. One particular solution of eq 10 is for $z = z_{\mathrm{L}}$

$$\frac{C^0_{\mathrm{OH}^-}x}{2C^{*,\mathrm{L}}_{\mathrm{CO}_2}} = k_{\mathrm{L}}a\frac{z_{\mathrm{L}}}{u^{\mathrm{L}}} = k_{\mathrm{L}}a\bar{t} \tag{11}$$

which allows one to calculate the values of $\beta_{\mathrm{L}} = k_{\mathrm{L}}a$ (the results are reported in Figure 9, in which the solid line accounts for the values of ΔP for incipient bubbles formation as a function of the liquid flow rates). Obviously, in this case, k_{L} contains the enhancement factor to be estimated. As can be seen from Figure 9, values of $k_{\mathrm{L}}a$ are much greater than those of $k_{\mathrm{L}}a$ evaluated for physical absorption (0.05 s^{-1}). To estimate the enhancement factor, the comparison must be made between runs performed in both cases, chemical and physical absorption, at the ΔP value of incipient bubbles formation. The values of the enhancement factor, calculated as the ratio between k_{L} obtained in chemical tests and k_{L} obtained in physical tests, are reported in Figure 10 for a specific value of the liquid flow rate. These results shed light on the interdependence between ΔP and the enhancement factor, which is positively affected by the possibility of increasing the ΔP value. In particular, values of the enhancement factor in the range of ∼4−8

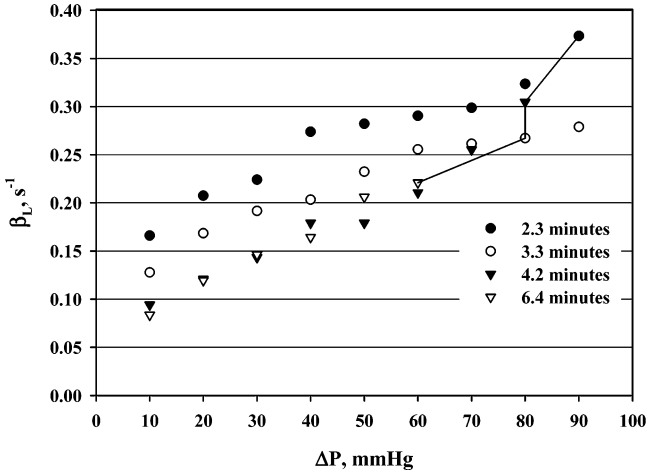

Figure 9. Overall mass transfer coefficient β_L for tests of the chemical absorption of CO_2 into a NaOH solution in the tubular reactor with a single membrane-tube as a function of the gas ΔP and the liquid mean residence time in the annulus.

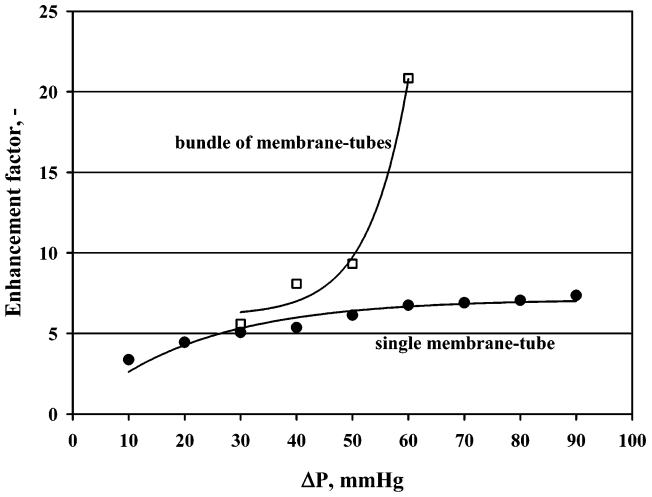

Figure 10. Estimation of the enhancement factor as a function of the ΔP for incipient bubbles formation for tests conducted in the tubular reactor with a single membrane-tube (liquid flow rate = 0.07 mL/s) and with a bundle of membrane-tubes (liquid flow rate = 1.79 mL/s).

have been obtained in the range of ΔP's under investigation (10−90 mmHg).

Tubular Reactor with a Bundle of Membrane-Tubes. Figure 11 reports the experimental results of physical absorption tests, in terms of $C^{L}_{O_2}$ as a function of the $\bar{t}$ of the water at the outlet of the shell. Also in this case, such as in the case of a single membrane-tube (cf. Figure 7), the lower the $\bar{t}$, the lower the $C^{L}_{O_2}$ (it is 2.6 ppm at 11 s and 8.1 ppm at 55 s). Data in Figure 11 were fitted by an "exponential-rise-to-maximum" function by taking into account the value of $C^{*,L}_{O_2}$ (8.5 ppm, cf. Figure 7). This value was employed in the calculus of $\beta_L = k_L a$ (eq 7) which resulted, for all tests, on the order of 4×10^{-2} s^{-1} (it is recalled here that, for this reactor, the specific interfacial area of the membrane system is 3.74 cm^{-1}). As can be observed, the use of a bundle of membrane-tubes instead of a single one did not result in any improvement in the mass transfer coefficient β_L, since the performances of the two systems were comparable.

Figure 12 shows the experimental results of chemical absorption tests of CO_2 in the NaOH solution, in terms of OH^- conversion (see eq 8) as a function of ΔP and $\bar{t}$.

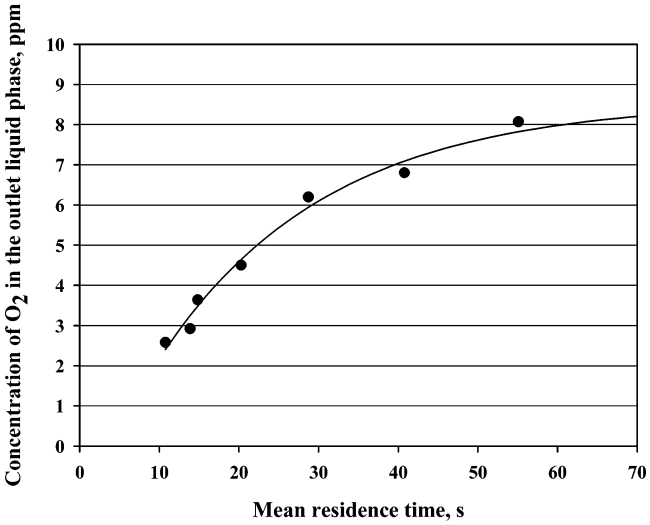

Figure 11. Values of outlet $C^{L}_{O_2}$ for tests of the physical absorption of O_2 into water in the tubular reactor with a bundle of membrane-tubes as a function of the water mean residence time in the shell (ΔP = 30 mmHg).

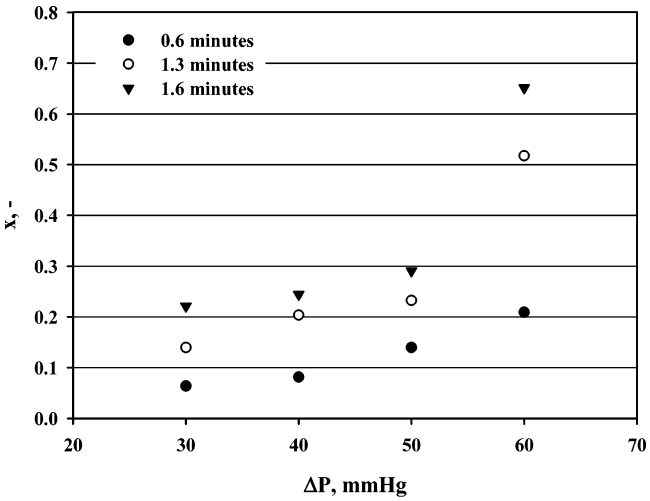

Figure 12. Values of x for tests of the chemical absorption of CO_2 into a NaOH solution in the tubular reactor with a bundle of membrane-tubes as a function of the gas ΔP and the liquid mean residence time in the shell.

By comparing these results with those obtained in the analogous tests conducted in the single-tube reactor (Figure 8), similar comments may be made: also in this case, x increases as both ΔP and $\bar{t}$ increase. Here, a narrower range of operating conditions was investigated; nevertheless, the differences among the tests are enhanced when the ΔP is sufficiently high (ΔP = 60 mmHg). Moreover, the longer $\bar{t}$ (1.6 min) yielded x as high as 65% (at ΔP = 60 mmHg), while the higher x-value obtained at $\bar{t}$ = 2.3 min in the single-tube reactor was only 44%: in that case, only the tests conducted at higher $\bar{t}$ were able to give x-values of 65% or more at a fixed ΔP. This sheds light on the better performance of a configuration with multiple membrane-tubes with respect to the simpler reactor examined in the previous case.

To quantitatively assess this, the same approach of eqs 9−11 was followed (Figure 13): with respect to Figure 9, again the mass transfer coefficient β_L increases when ΔP increases. Nevertheless, it was not possible to estimate a clear dependence of β_L on $\bar{t}$, but the generally higher values of β_L are evident: β_L reached

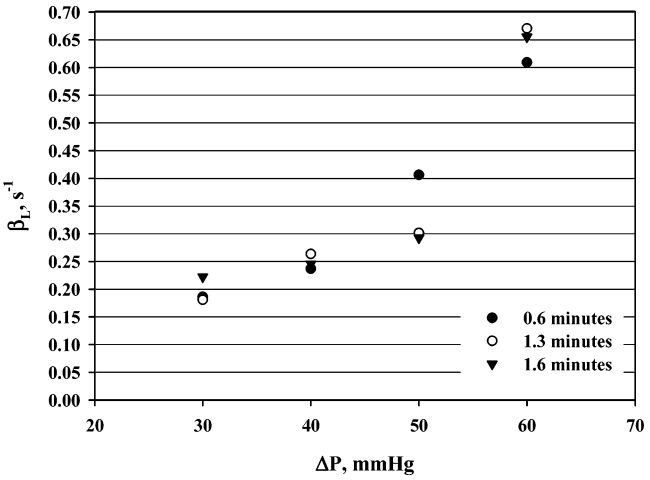

Figure 13. Overall mass transfer coefficient β_L for tests of the chemical absorption of CO_2 into a NaOH solution in the tubular reactor with a bundle of membrane-tubes as a function of the gas ΔP and the liquid mean residence time in the shell.

$\sim$0.65 s^{-1} at ΔP = 60 mmHg, figures never obtained with the single-tube reactor. Again, the enhancement factor was estimated as done in the case of the reactor with a single membrane-tube, and the results are reported in Figure 10: also in this case, there is clear evidence of the positive effect that ΔP has on the enhancement factor. In particular, values of the enhancement factor in the range of $\sim$5−21 have been obtained in the range of ΔP's under investigation (30−60 mmHg).

Conclusions

In this work, it has been shown that the use of opportunely designed membrane laboratory reactors allows one to study the gas−liquid mass transfer phenomena in a more controlled way. In fact, by using porous membranes and by applying a proper gas differential pressure ΔP, a well-defined and constant interfacial area, which can be changed simply by increasing or reducing the number of membranes to be used, is obtained.

In particular in the present work, the behavior of a gas−liquid contactor was compared when used for physical and for chemical absorption (in the presence of a very fast reaction). In the second case, to satisfy the gaseous reactant demand, the ΔP necessary for incipient gas bubble formation had to be increased. This means that, in the presence of a very fast reaction, a higher gas flow rate was needed, and this can be obtained, when using a membrane, only by increasing the ΔP of the gas across the pores. Actually, if the same value of ΔP is used in the absence or in the presence of a very fast chemical reaction, the gas mass transfer rates are comparable in the two cases. Namely, an enhancement factor equal to $\sim$1 was obtained, which is unrealistic. On the other hand, by increasing the ΔP value in the presence of a chemical reaction, no incipient bubble formation is observed up to a value at which the mass transfer rate is equal to the reaction rate. This is confirmed by the experimental observation that the pressure of the liquid necessary for filling or evacuating the pores, for the used membranes, is $\sim$1.5 bar against the atmosphere, that is, much higher than the ΔP's adopted in the present investigation. This means that, in all the considered cases, the pores were filled only with the gas, and the mass transfer was located at the liquid-side pores mouth. The greater ΔP necessary for producing bubbles in the presence of a fast reaction is only due to the rapid consumption of the gaseous reactant, that is, as mentioned before, the gas flow rate must be increased in order to supply enough reactant to satisfy the reaction rate requirement. Altogether, the simple ΔP and gas flow rate measurements, respectively, performed in the absence and the presence of a chemical reaction, give an experimental estimation of the enhancement factor, as shown in the paper.

By using membranes in gas−liquid reactors for dosing the gaseous reagent, it is possible, by changing the ΔP value, to feed exactly the amount of gas necessary to the reaction, provided that the extension of the membrane external surface is enough for the scope. Otherwise, it is possible to change the number of membrane-tubes or their length, remembering, as observed, that the mass transfer rate is roughly proportional to the external surface area of the membranes. This gives suggestions for both the scale-down for laboratory miniaturized devices and the scale-up for gas−liquid and gas−liquid−solid industrial reactors and also for the development of modular membrane contactors. Finally, it is highlighted that the results obtained in this work could also be extended to a gas−liquid−solid membrane contactor, in which a solid is suspended in the liquid phase and the membrane allows the contact between the gas and the liquid.

List of Symbols

a = specific liquid/gas interfacial area, cm^{-1}
β_L = overall volumetric mass transfer coefficient, s^{-1}
C_{CO_2} = CO_2 concentration, ppm
C_{O_2} = O_2 concentration, ppm
C_{OH^-} = OH^- concentration, ppm
ΔP = pressure difference between the inlet gas and the reactor, mmHg
k_L = mass transfer coefficient in the liquid phase, cm/s
N = rate of O_2 chemically absorbed, mL/s
t = time, s
$\bar{t}$ = liquid mean residence time, s
u = axial velocity, cm/s
x = degree of OH^- conversion
z = tubular reactor axis, cm
z_L = length of the tubular reactor, cm

Superscripts

0 = inlet value
* = equilibrium value
L = liquid

Subscripts

i = generic value
ref = reference value

Note Added after ASAP Publication. This article was released ASAP on June 1, 2005, with errors in the sub- and superscripts in eqs 8−11. The version posted on June 21, 2005, and the printed version are correct.

Literature Cited

(1) Armor, J. N. Membrane catalysis: where is it now, what needs to be done? *Catal. Today* **1995**, *25*, 199.

(2) Gabelman, A.; Hwang, S. T. Hollow fiber membrane contactors. *J. Membr. Sci.* **1999**, *159*, 61.

(3) Vospernik, M.; Pintar, A.; Berčič, G.; Levec, J. Mass transfer studies in gas−liquid−solid membrane contactors. *Catal. Today* **2003**, *79*−*80*, 169.

(4) Karoor, S.; Sirkar, K. K. Gas absorption studies in microporous hollow fiber membrane modules. *Ind. Eng. Chem. Res.* **1993**, *32*, 674.

(5) Mavroudi, M.; Kaldis, S. P.; Sakellaropoulos, G. P. Reduction of CO_2 emissions by a membrane contacting process. *Fuel* **2003**, *82*, 2153.

(6) Yang, M. C.; Cussler, E. L. Designing hollow-fiber contactors. *AIChE J.* **1986**, *32*, 1910.

(7) Daiminger, U. A.; Geist, A. G.; Nitsch, W.; Plucinski, P. K. Efficiency of hollow fiber modules for nondispersive chemical extraction. *Ind. Eng. Chem. Res.* **1996**, *35*, 184.

(8) Liu, S. H.; Luo, G. S.; Wang, Y.; Wang, Y. J. Preparation of coiled hollow-fiber membrane and mass transfer performance in membrane extraction. *J. Membr. Sci.* **2003**, *215*, 203.

(9) Kumar, P. S.; Hogendoorn, J. A.; Feron, P. H. M.; Versteeg, G. F. Approximate solution to predict the enhancement factor for the reactive absorption of a gas in a liquid flowing through a microporous membrane hollow fiber. *J. Membr. Sci.* **2003**, *213*, 231.

(10) Wang, R.; Li, D. F.; Liang, D. T. Modeling of CO_2 capture by three typical amine solutions in hollow fiber membrane contactors. *Chem. Eng. Process.* **2004**, *43*, 849.

(11) Rangwala, H. A. Absorption of carbon dioxide into aqueous solutions using hollow fiber membrane contactors. *J. Membr. Sci.* **1996**, *112*, 229.

(12) Tsou, D. T.; Blachman, M. W.; Davis, J. C. Silver-facilitated olefin/paraffin separation in a liquid membrane contactor system. *Ind. Eng. Chem. Res.* **1994**, *33*, 3209.

(13) Zhu, Y.; Minet, R. G.; Tsotsis, T. T. A continuous pervaporation membrane reactor for the study of esterification reactions using a composite polymeric/ceramic membrane. *Chem. Eng. Sci.* **1996**, *51*, 4103.

(14) Ferreira, B. S.; Fernandes, H. L.; Reis, A.; Mateus, M. Microporous hollow fibres for carbon dioxide absorption: mass transfer model fitting and the supplying of carbon dioxide to microalgal cultures. *J. Chem. Technol. Biotechnol.* **1998**, *71*, 61.

(15) Coronas, J.; Santamaría, J. Catalytic reactors based on porous ceramic membranes. *Catal. Today* **1999**, *51*, 377.

(16) Linek, V.; Vacek, V. Chemical engineering use of catalyzed sulfite oxidation kinetics for the determination of mass transfer characteristics of gas−liquid contactors. *Chem. Eng. Sci.* **1981**, *36*, 1747.

(17) Astarita, G. *Mass Transfer with Chemical Reaction*; Elsevier: Amsterdam, The Netherlands, 1967.

(18) Perry, R. H.; Green, D. W. *Perry's Chemical Engineers' Handbook*; McGraw-Hill: New York, 1998.

Received for review February 22, 2005
Revised manuscript received May 3, 2005
Accepted May 4, 2005

IE050226G